

Solvent Dependent Conformational Relaxation of *cis*-1,3,5-HexatrieneD. Ahmadi Harris,<sup>†</sup> Michael B. Orozco,<sup>‡</sup> and Roseanne J. Sension<sup>†,‡,§,\*</sup>

FOCUS Center, Department of Chemistry, and Program in Applied Physics, University of Michigan, Ann Arbor, Michigan, 48109-1055

Received: March 7, 2006; In Final Form: May 31, 2006

Ultrafast transient absorption spectroscopy was used to study the conformational relaxation dynamics of 1,3,5-*cis*-hexatriene (Z-HT) produced in the photochemical ring-opening reaction of 1,3-cyclohexadiene (CHD) in methanol and *n*-propanol solvents. The results are compared with earlier investigations performed using cyclohexane and hexadecane solvents [Anderson, N. A.; Pullen, S. H.; Walker II, L. A.; Shiang, J. J.; Sension, R. J.; *J. Phys. Chem. A* **1998**, *102*, 10588–10598.]. The conformational relaxation between hot cZc-HT, cZt-HT, and tZt-HT, where the labels c and t designate *cis* and *trans* configurations about the single bonds, is much faster in alcohol solvents than in alkane solvents. The hot Z-HT produced in the photochemical ring-opening reaction evolves from the conformationally strained cZc-HT form to the more stable cZt-HT form on a time scale of 2 ps in alcohols compared with 6 ps in alkanes. The overall decay of the internal vibrational temperature of the hot Z-HT is faster in alcohols (5–6 ps) than alkanes (12–20 ps) and is weakly dependent on the specific alcohol or alkane solvent. A small population of cZt-HT (5–10%) is trapped as the solute equilibrates with the surrounding solvent following UV excitation of CHD or direct UV excitation of Z-HT. The influence of solvent on conformational relaxation of Z-HT was investigated further by probing the temperature dependence of the decay of this thermally equilibrated cZt-HT population. The apparent barrier for the cZt → tZt conformational isomerization is lower in alcohols (17.4 kJ/mol) than in alkanes (23.5 kJ/mol). However the equilibrium Arrhenius prefactor ( $A_0$ ) is an order of magnitude smaller for alcohols (ca.  $4 \times 10^{12}$ ) than alkanes (ca.  $6 \times 10^{13}$ ) resulting in an absolute rate of decay that is faster in the alkane than in the alcohol solvents. These results are discussed in the context of transition state theory and Kramers' theory for condensed phase reaction dynamics.

## I. Introduction

Solvent–solute interactions play a vital role in chemical reactions by influencing the reactivity of, and energy flow within, the species involved. The ring-opening reaction of 1,3-cyclohexadiene (CHD) and subsequent relaxation of hot 1,3,5-*cis*-hexatriene (Z-HT) provides an interesting paradigm for the detailed investigation of energy flow in a chemical system. Several groups have investigated both the electrocyclic ring-opening reaction of CHD,<sup>1–26</sup> and of the related 7-dehydrocholesterol chromophore responsible for the photoreaction that results in vitamin D formation.<sup>27–31</sup> Initial UV excitation of CHD produces a population in the  $1^1B$  state which decays by internal conversion to an optically forbidden  $2^1A$  state on a time scale of ca. 10 fs.<sup>4,31</sup> The electrocyclic ring-opening reaction of CHD occurs on the  $2^1A$  state and produces vibrationally hot *cis*-1,3,5-hexatriene with a quantum yield of 0.40.<sup>1</sup> A cartoon illustrating this process is sketched in Figure 1.

Upon ground-state recovery following photoinitiation of the ring-opening reaction, rapid interconversion among the three conformers of HT produces a dynamic equilibrium mixture of cZc-HT, cZt-HT, and tZt-HT (where the labels c and t designate *cis* (or more precisely *gauche*) and *trans* configurations about the single bonds). As the molecules relax, the mixture evolves

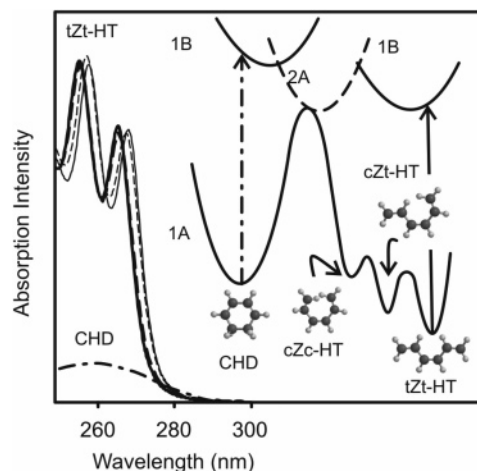


**Figure 1.** (left) Ground-state absorption spectra of CHD in cyclohexane (dot-dashed line) and Z-HT in cyclohexane (thin dashed line), hexadecane (thin solid line), methanol (thicker solid line), and 1-propanol (thicker dashed line). The spectrum of CHD does not change significantly with solvent. (right) Cartoon of relevant potential energy surfaces for the CHD ring-opening reaction.

in composition and deposits energy into the surrounding solvent. Thermal equilibration with the solvent occurs on a time scale of 10–20 ps, leaving a small population of cZt-HT molecules trapped for a period >100 ps by the barrier for single bond isomerization to tZt-HT.

The ground-state relaxation of hot Z-HT was analyzed by Anderson et al. using a time dependent molecular temperature

\* To whom correspondence should be addressed. E-mail: rsension@umich.edu.

<sup>†</sup> FOCUS Center.

<sup>‡</sup> Department of Chemistry.

<sup>§</sup> Program in Applied Physics.

in the context of Kramers' theory for barrier-crossing processes.<sup>17,32</sup> These studies demonstrated that the rate of relaxation is essentially independent of the macroscopic solvent shear viscosity ( $\eta$ ), with little difference in the rate measured in cyclohexane ( $\eta = 0.894$  mPa s, 25 °C)<sup>33</sup> and hexadecane ( $\eta = 3.032$  mPa s, 25 °C) solvents. In contrast the relaxation observed by Lochbrunner et al. in ethanol ( $\eta = 1.074$  mPa s, 25 °C) is approximately four times faster than in the alkanes.<sup>17,20</sup> In addition, the absolute magnitude of the trapped cZt-HT population is lower in ethanol than in the alkanes. These results posed a conundrum as solvent polarity is expected to have little influence on the barrier for single bond isomerization and the typical mode of interaction in a barrier crossing process is correlated with the solvent friction and thus the solvent viscosity.

In this paper, we will consider the influence of solvent on the ring-opening reaction of CHD and the conformational relaxation of Z-HT in more detail. These studies will investigate the ring-opening reaction in methanol and *n*-propanol for comparison with the earlier studies in cyclohexane, hexadecane, and ethanol, and will use temperature as a tool to explore the influence of solvent on the ground-state barrier for the cZt-HT  $\rightarrow$  tZt-HT conformational isomerization.

## II. Experimental Methods

Pump–probe transient absorption experiments were performed using 0.3 mJ laser pulses from a home-built 1 kHz titanium-sapphire laser system. CHD (Aldrich 95%) samples were prepared in solution to have an optical density of approximately 1 at 267 nm for a 1-mm sample thickness. A pump and flow cell were used to refresh the sample volume between laser shots. The sample was excited at 267 nm with the output of a third harmonic generation setup consisting of two cascaded nonlinear stages: second harmonic generation followed by sum frequency generation. Following the second harmonic generation crystal, the fundamental beam and the second harmonic were separated using a dichroic mirror. The relative timing of the two beams was adjusted to ensure good temporal overlap and a second dichroic mirror recombined the beams for collinear sum frequency mixing in a  $\beta$ -BaB<sub>2</sub>O<sub>4</sub> (BBO) crystal. A fused silica prism pair was used for subsequent pulse recompression.<sup>31</sup>

For transient absorption kinetic measurements, a tunable ultraviolet probe pulse was generated by producing the second harmonic of a visible noncollinear optical parametric amplifier (NOPA) in a BBO crystal. A 150-mm computer-controlled translation stage with 0.1- $\mu$ m step size was used to control the time delay between the pump and probe pulses. For measurements of the transient difference spectrum, a broadband ultraviolet probe was generated by focusing the fundamental of the Ti:sapphire laser into a 1-cm cell of ethylene glycol where self-phase modulation broadened the spectrum into a white light continuum. The white light was collimated and focused by a fast achromatic lens ( $f = 30$  mm) into a BBO crystal for type I doubling. Typically, a bandwidth of ca. 80 nm of visible radiation was adequately phase-matched for second harmonic generation producing a spectral continuum spanning the region from 260 to 300 nm. In all measurements the pump and probe polarizations were oriented at magic angle (54.7°) with respect to each other to eliminate the influence of rotational relaxation, allowing for the direct observation of the population relaxation.

In addition to measurements of Z-HT formed in the CHD ring-opening reaction, direct excitation of Z-HT was used to produce cZt-HT. Excitation of Z-HT increases the yield (100% of excited molecules form hot HT as opposed to 40% following excitation of CHD) and reduces background contributions to

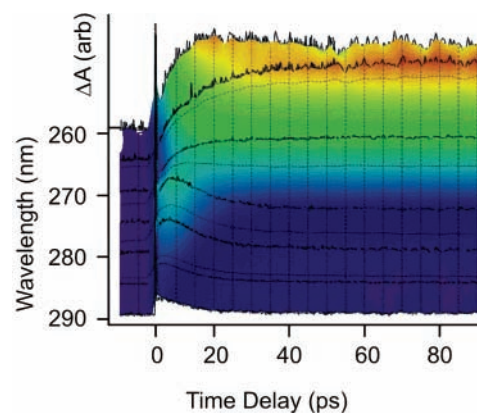


**Figure 2.** Transient absorption kinetics of CHD in propanol following excitation at 266 nm. The individual traces are plotted as dark lines with a surface plot representation of the evolving spectrum superimposed.

the transient absorption signal. For these measurements, Z-HT was synthesized as a mixture of the E-HT and Z-HT isomers according to the method described by Hwa et al.<sup>34</sup> The Z-HT isomer was isolated from the mixture by reaction of the trans isomer with maleic anhydride.<sup>34</sup>

One color ( $\lambda_{\text{pump}} = \lambda_{\text{probe}} = 266$  nm) transient absorption kinetics traces were obtained for Z-HT as a function of temperature. The pump pulse was produced as described above. The probe pulse was obtained by sending a portion of the 800-nm fundamental laser beam onto a 1.5-m computer-controlled delay stage. This delay stage permits accurate measurements spanning six decades in time from 10 fs to 10 ns. The third harmonic was generated by using back-to-back BBO crystals after the stage. The first crystal is used for second harmonic generation, and the second crystal produces the third harmonic through sum frequency generation. The 800-nm beam was carefully aligned on the delay stage to ensure that the pulse energy of the third harmonic probe was the same when the retro-reflector was at the back of the stage and at the front of the stage. Again the pump and probe polarizations were oriented at magic angle (54.7°) with respect to each other to eliminate the influence of rotational relaxation, allowing for the direct observation of the population relaxation.

Temperature control was achieved by immersing the sample reservoir in a bath with a 50/50 mixture of water and ethylene glycol. The temperature of the bath was controlled by a Neslab RTE-111 refrigerated bath/circulators, capable of maintaining temperatures from  $-25$  to  $+150$  °C. The sample was flowed with a peristaltic pump, and the temperature was measured with a temperature probe inserted in a T-joint located immediately after the sample cell. The temperatures of the solvents were varied from 15 to 70 °C in cyclohexane, 21 to 80 °C in hexadecane, 10 to 56 °C in methanol, and 10 to 76 °C in *n*-propanol. The temperature was maintained with an accuracy of  $\pm 0.5$  °C.

## III. Results

**Relaxation of Z-HT Following Photoinitiated Ring-Opening.** Transient absorption data were obtained for the ring-opening reaction of CHD in methanol and *n*-propanol solvents. Kinetic traces were obtained at probe wavelengths of 260, 265, 270, 275, 280, 285, and 290 nm. These traces were normalized in intensity by using transient spectra obtained at time delays of 5, 10, and 20 ps and the steady state difference spectrum expected at long time delays. The data obtained in propanol are summarized in Figure 2. The data obtained in methanol are similar.

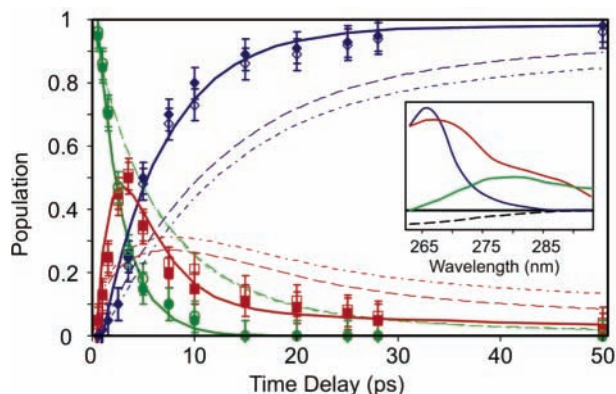


**Figure 3.** The calculated population dynamics of Z-HT conformers following CHD ring opening are shown for the methanol solvent (filled) and propanol solvent (open). The conformers are denoted by blue diamonds (tZt-HT), red squares (cZt-HT), and green circles (cZc-HT). The solid line denotes the fit to the dynamics in the alcohol solvents. The dashed line denotes the fit to the dynamics in cyclohexane, and the dot-dashed line denotes the fit to the dynamics in hexadecane as reported previously.<sup>17</sup> The three basis spectra for cZc, cZt, and tZt are illustrated in the inset with the same color code. The black dashed line is the spectrum of the CHD bleach.

These transient absorption data detail ground-state recovery and reveal the conformational dynamics of Z-HT following the ring-opening reaction of CHD. The conformer population dynamics were extracted from the transient absorption data using eq 1 as described earlier for the evolution in alkane solvents<sup>17</sup>

$$\Delta A(t, \lambda) = \Phi_{cZc}(t)A_{cZc}(\lambda) + \Phi_{cZt}(t)A_{cZt}(\lambda) + \Phi_{tZt}(t)A_{tZt}(\lambda) - A_{\text{CHD}}(\lambda) \quad (1)$$

where the  $\Phi(t)$  represent the conformer populations as a function of time with the constraint  $\Phi_{cZc}(t) + \Phi_{cZt}(t) + \Phi_{tZt}(t) = 1$ , and  $A_{cZc}$ ,  $A_{cZt}$ ,  $A_{tZt}$ , and  $A_{\text{CHD}}$  are the absorption spectra of cZc-HT, cZt-HT, tZt-HT, and CHD, respectively.

The normalized conformer population dynamics of HT following the CHD ring-opening reaction in both alkane and alcohol solvents are compared in Figure 3. The three basis spectra for cZc, cZt, and tZt in the alcohols are shown in the inset to Figure 3. These are similar to those reported earlier for alkanes, although blue shifted by ca. 2 nm. The tZt spectrum is the steady-state spectrum, the cZt spectrum is derived from the long time absorption following excitation of Z-HT or CHD, and the cZc spectrum is deduced from the earliest time behavior following excitation of CHD.<sup>17</sup> The analysis is not very sensitive to the details of these spectra but reflects the fact that cZc absorbs to the red, tZt absorbs to the blue, and cZt absorbs both on the red and blue sides of the observation window.

The mixture of conformers has a more rapid evolution in the alcohol solvents than in alkane solvents. This is marked both by a faster decay of cZc-HT and a faster growth of tZt-HT in alcohols and, as a larger transient population of the intermediate conformer, cZt-HT. At long times (>50ps), the trapping of the cZt-HT population is diminished in the alcohol solvents compared to the alkane solvents. In the alcohol solvents the cZc-HT population disappears with a time constant of  $2 \pm 1$  ps. The cZt-HT population appears with a time constant of  $2.1 \pm 1$  ps and disappears with a time constant of  $6 \pm 1$  ps. The tZt-HT population rises with a time constant of  $6 \pm 1$  ps. The decay of cZc-HT and rise of (cZt-HT + tZt-HT) is somewhat slower than that extracted from the observations reported by Lochbrunner et al. in ethanol solvent, ca. 2 ps rather than ca. 1

ps.<sup>20</sup> Nonetheless, the relaxation is much faster in the alcohols than the corresponding relaxation in cyclohexane or hexadecane.<sup>17</sup>

**Ground-State Barrier for cZt-HT  $\rightarrow$  tZt-HT Isomerization.** The ground state conformer dynamics summarized above show an obvious dependence on solvent but a significant lack of dependence on the solvent viscosity. At 25 °C the viscosities ( $\eta$ ) of the two alcohol solvents investigated here are 0.544 mPa s (methanol) and 1.945 mPa s (propanol) compared with 0.894 mPa s (cyclohexane) and 3.032 mPa s (hexadecane) for the two alkanes solvents studied earlier.<sup>33</sup> The trend between the two alcohols (methanol slightly faster than propanol) and between the two alkanes (cyclohexane faster than hexadecane) follow the trend anticipated from viscosity, but the differences are small and not consistent with the  $\eta^{-1}$  dependence deduced from simple application of Kramers' theory, as described in more detail below. The solvent dependence observed may arise from a dynamic interaction of the solute with the solvent as HT relaxes to thermal equilibrium. Alternatively, the solvent dependence may arise from an intrinsic dependence of the barrier for single bond isomerization on the solvent polarity. Both the increased rate of single bond isomerization and the diminished trapping of the cZt-HT population with increased solvent polarity are consistent with stabilization of the barrier for single bond isomerization in the more polar solvents.

The long time transient absorption signal observed following excitation of CHD details the trapping of the ground state cZt-HT population following formation of Z-HT. Direct observation of cZt-HT population dynamics may also be obtained by measuring the ground state recovery of initially excited Z-HT, instead of initially excited CHD. This measurement provides a clearer measure of the relaxation by increasing the yield (100% of excited molecules form hot HT as opposed to 40% following excitation of CHD) and reducing background contributions to the signal.

One-color ( $\lambda_{\text{pump}} = \lambda_{\text{probe}} = 266$  nm) transient absorption kinetics traces were obtained for Z-HT in cyclohexane, hexadecane, propanol, and methanol as a function of temperature between 10 and 80 °C to observe the effect of solvent polarity on the ground state conformational relaxation of Z-HT. A typical trace is shown in Figure 4.

The ground-state recovery shows two distinct temporal regions. The fast component (<50 ps) corresponds to the thermalization of hot Z-HT following internal conversion from the excited electronic state. This component is essentially independent of the bulk solvent temperature. The slower component (>50 ps) corresponds to the decay of the population of the trapped cZt-HT conformer after thermalization with the surrounding solvent. The rate of decay of this latter component is strongly dependent on the temperature of the bulk solution. The transient absorption traces for times longer than 40 or 50 ps were well modeled by a single-exponential decay. These data can be analyzed using an Arrhenius type equation for the rate constant

$$k = A_{\text{h}} e^{-E_{\text{a}}/RT} \quad (2)$$

An activation energy barrier height for the cZt-HT  $\rightarrow$  tZt-HT transition may be extracted from the slope of a plot of  $\ln(k)$  vs  $1/T$

$$\ln(k) = \frac{-E_{\text{a}}}{RT} + \ln(A_{\text{h}}) \quad (3)$$

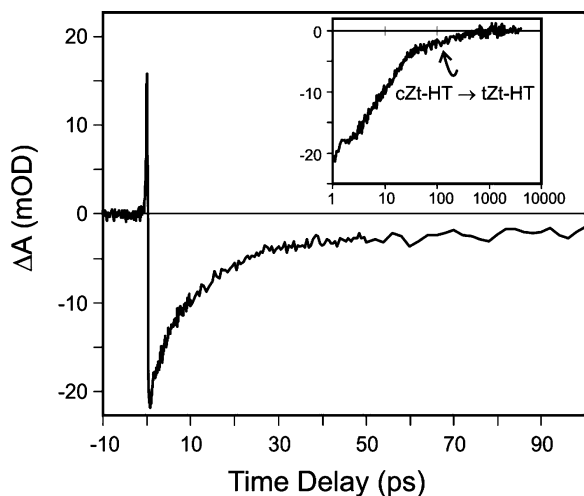


**Figure 4.** Transient absorption kinetics of Z-HT in methanol at 19 °C. The rapid (<50 ps) bleach recovery is independent of the solvent temperature over the temperature range studied, but the long time (>50 ps) residual recovery displays a notable temperature dependence. The data in the inset is plotted on a logarithmic time scale to highlight the temperature dependent component corresponding to the slow relaxation of trapped cZt-HT.

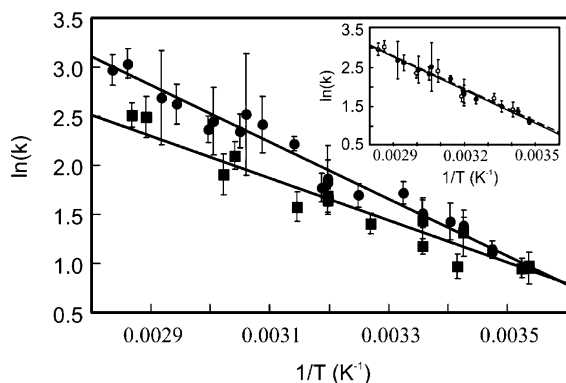


**Figure 5.** Weighted linear least-squares fit of the rate constants ( $\text{ns}^{-1}$ ) as a function of temperature to eq 3. The best fit parameters are: alcohols (squares),  $E_a = 17.2 \pm 2.4$  kJ/mol,  $A_h = 3.8 (-2.3, +6.2) \times 10^{12}$   $\text{s}^{-1}$ ; alkanes (circles),  $E_a = 23.5 \pm 2.5$  kJ/mol,  $A_h = 6.0 (-3.8, +10.1) \times 10^{13}$   $\text{s}^{-1}$ . The error ranges are calculated as the standard uncertainties in a weighted least-squares fit. The inset shows a comparison of the fits for hexadecane (open circles, dashed line) and cyclohexane (filled circles, solid line) separately.

These linear fits to the data are plotted in Figure 5. It is important to note, however, that the errors are not constant and a weighted least-squares method must be used to extract accurate values and error estimates for  $E_a$  and  $A_h$ . Fits obtained for the two alkane solvents are indistinguishable within the scatter of the data (see the inset in Figure 5). The same is true of the alcohol solvents, although the data sets are smaller, and the scatter is larger, resulting in a greater uncertainty in the parameters of the fit. In the analysis that follows the data obtained in both alcohols will be grouped together as will the data obtained in both alkanes.

An activation energy barrier height for the cZt-HT  $\rightarrow$  tZt-HT transition may also be extracted directly via a nonlinear fit to eq 2. Fits to the data in both alkane and alcohol solvents are plotted in Figure 6. In both cases the reduced chi-squared ( $\chi_r^2$ ) for the best fit is near 1 (1.0815 in alcohols and 0.8343 in alkanes). The range of values for the parameters  $A_h$  and  $E_a$  consistent with the data are highly correlated. These ranges are illustrated in the form of contour plots of  $\chi_r^2(A_h, E_a)$  in Figure 7.

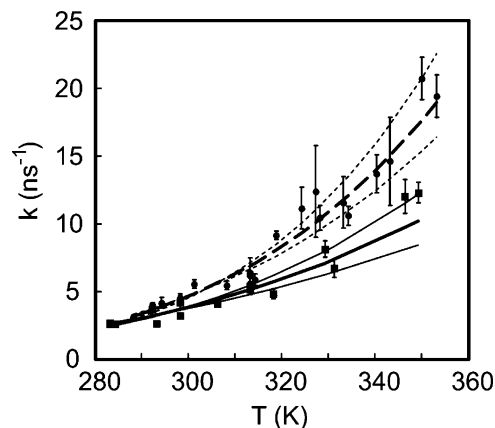


**Figure 6.** Fits of the rate constants obtained for the cZt  $\rightarrow$  tZt isomerization to an Arrhenius expression. Circles and dashed curves are the rates in alkanes, while the squares and solid curves are the rates in alcohols. The thin lines represent the ranges calculated using parameters for  $A_h$  and  $E_a$  for which  $\chi_r^2 \leq \chi_r^2(\text{min}) + 0.2$ . The best fit parameters are alcohols,  $E_a = 17.4$  kJ/mol,  $A_h = 4.1 \times 10^{12}$   $\text{s}^{-1}$ ; alkanes,  $E_a = 23.2$  kJ/mol,  $A_h = 5.2 \times 10^{13}$   $\text{s}^{-1}$ .

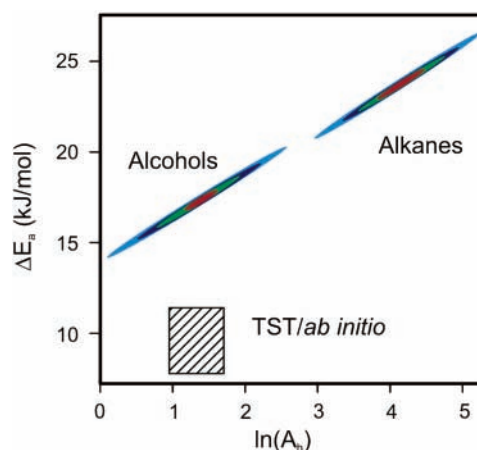


**Figure 7.** Contour plot of  $\chi_r^2$  as a function of the fit parameters  $A_h$  and  $E_a$  for the data obtained in alcohols and alkanes. The contours are: red,  $\chi_r^2$  within 0.01 of the minimum; green,  $\chi_r^2$  within 0.05 of the minimum; dark blue,  $\chi_r^2$  within 0.1 of the minimum; light blue,  $\chi_r^2$  within 0.2 of the minimum. The dashed box represents the range of barriers calculated as described in the text and the range for  $A_h$  calculated using transition-state theory. The dark blue ellipses are essentially equivalent to the error ranges obtained in the weighted linear least-squares fit.

From this data set it is clear that the relaxation of cZt-HT in thermal equilibrium with the solvent is consistently faster in the alkane solvents than in the alcohol solvents. This is in striking contrast to the observation for the hot HT initially formed following excitation of CHD where relaxation in alcohols is faster than in alkanes. It is also noteworthy that within the scatter of the data set there is no significant dependence on the specific alcohol or alkane solvent. The effective barrier for the cZt-HT  $\rightarrow$  tZt-HT single bond isomerization in the alkane solvents ( $23.5 \pm 2.5$  kJ/mol) is higher than the effective barrier in alcohol solvents ( $17.2 \pm 2.4$  kJ/mol). The Arrhenius prefactor is an order of magnitude smaller in alcohol solvents,  $A_h = 4 \times 10^{12}$   $\text{s}^{-1}$ , than in alkane solvents,  $A_h = 6 \times 10^{13}$   $\text{s}^{-1}$ .

#### IV. Discussion

**Comparison of the cZt  $\rightarrow$  tZt-HT Barrier with Other Calculations and Experiments.** The activation barriers reported above for the cZt  $\rightarrow$  tZt isomerization are in reasonable

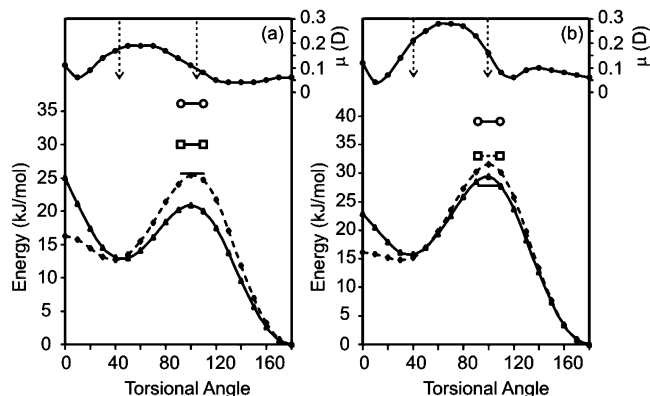


**Figure 8.** Calculated torsional potentials for the  $c \rightarrow t$  isomerization of 1,3-butadiene (dashed line, diamonds) and the  $cZt \rightarrow tZt$  isomerization of 1,3,5-hexatriene (solid line, triangles) (a) RHF 6-31G\* and (b) B3LYP/6-31G\*\*. The angle is defined as  $0^\circ$  in the *cis* configuration and  $180^\circ$  in the *trans* configuration. The horizontal lines represent the experimental barriers for  $c \rightarrow t$  isomerization, butadiene vapor (no endcaps), Z-HT in alcohols (square endcaps), and Z-HT in alkanes (circle endcaps). The calculated dipole moment (circles) is plotted along the scale on the right axis for each method. The vertical dashed arrows indicate the approximate positions of the  $cZt$  minimum (ca.  $40^\circ$ ) and the  $cZt \rightarrow tZt$  transition state (ca.  $100^\circ$ ).

agreement with similar measurements reported in the literature for other polyenes. The barrier for the  $cEtEt \rightarrow tEtEt$  single bond isomerization of *trans*-octatetraene was determined by photoproduction of  $cEtEt$  and thermal recovery of the  $tEtEt$  ground state at low temperature in an alkane matrix.<sup>35</sup> In this experiment the disappearance of the  $cEtEt$  conformer was monitored at six temperatures between 49 and 53 K. The data were fit to an Arrhenius expression, eq 2, yielding a barrier of  $16.4 \pm 0.8$  kJ/mol. A somewhat lower barrier has been deduced for butadiene from high-resolution Raman spectra of overtone torsional vibrations in the gas phase (13 kJ/mol for  $g \rightarrow t$ ).<sup>36</sup> Finally, it should be noted that this barrier is similar to the barrier reported for the related  $cZc \rightarrow cZt$  isomerization of previtamin D in ethanol ( $15.5 \pm 1$  kJ/mol).<sup>28</sup>

A few calculations of the  $cZt \rightarrow tZt$  isomerization of hexatriene have been reported in the literature. A barrier of 8.6 kJ/mol ( $720$   $\text{cm}^{-1}$ ) was obtained from a restricted Hartree–Fock (RHF) (6-31G) calculation reported earlier,<sup>26</sup> while a slightly higher barrier of 13.6 (11.2 with zero point correction) kJ/mol was reported for a calculation using density functional theory (DFT) (B3LYP/6-31G\*\*) methods.<sup>22</sup> These calculated barriers are much smaller than the experimentally determined effective barriers for Z-HT.

In contrast to a paucity of calculations of Z-HT, butadiene has provided an important test case for torsional potentials of conjugated polyenes. Several careful calculations have been reported recently comparing a variety of computational methods.<sup>37,38</sup> Calculated barriers range from 10.3 to 16.8 kJ/mol with the most accurate calculations providing a reasonable estimate within  $\pm 2$  kJ/mol of the 13 kJ/mol experimental barrier. Even a simple RHF 6-31G\* calculation does a qualitatively good job of reproducing the potential.

Torsional potentials for single bond isomerization in 1,3-butadiene and  $cZt \rightarrow tZt$ -HT are plotted in Figure 8. These potentials were calculated using the RHF 6-31G\* *ab initio* method and the B3LYP/6-31G\*\* density functional method with optimization of all other coordinates at each constrained value of the torsional angle. All calculations were performed using Spartan 04 (Wavefunction, Inc. Irvine CA). The *trans* configuration is defined as  $180^\circ$ , while the *cis* configuration is defined

as  $0^\circ$ . The torsional potential for butadiene is in good agreement with the HF calculation reported by Fabiano and Della Sala,<sup>38</sup> in qualitative agreement with the other calculations reported, and in excellent, although somewhat fortuitous, agreement with the experimental barrier. In contrast to the experimental observation on Z-HT however, this RHF 6-31G\* calculation predicts a lower barrier for  $cZt \rightarrow tZt$ -HT isomerization in hexatriene than for  $c \rightarrow t$  isomerization in butadiene. The B3LYP density functional calculation predicts a higher barrier for the  $c \rightarrow t$  isomerization for both butadiene and hexatriene, in good agreement with the results both of Fabiano and Della Sala for butadiene<sup>38</sup> and of Henseler et al. for hexatriene.<sup>21,22</sup>

The dependence of torsional barriers on environment and on environmental friction has been the subject of many investigations. Most of these studies have dealt with the motion of groups much larger than the  $\text{C}=\text{CH}_2$  group displaced in the single bond isomerizations reactions described here. In particular, the excited-state isomerization of *trans*-stilbene has been the subject of exhaustive investigation.<sup>39–57</sup> The effective barrier obtained from Arrhenius plots of the *trans*-stilbene lifetime in a series of alkanes contains a contribution arising from the activation energy for viscous flow acting as a friction on the reaction coordinate. Sun and Saltiel have reported a careful comparison of the excited state  $trans \rightarrow p$  isomerization of stilbene and determined that the intrinsic barrier for isomerization in alkanes was independent of solvent,  $\Delta H_t = 11.9$  kJ/mol.<sup>49</sup> If a torsional frequency of ca.  $100$   $\text{cm}^{-1}$  is assumed, the transition-state barrier is 13.8 kJ/mol (*vide infra*),<sup>50</sup> in good agreement with the gas-phase value of ca. 14 kJ/mol. Extensive investigations by Troe and co-workers have also identified minimal medium effects on excited-state torsional barriers in low viscosity nonpolar solvents for a broad range of stilbene and diphenylbutadiene derivatives.<sup>57</sup>

While the excited-state isomerization of *trans*-stilbene is in many respects similar to the  $cZt \rightarrow tZt$  isomerization of hexatriene, there are distinct differences as well. The hexatriene molecule is smaller than *trans*-stilbene, and the reorientational diffusion is faster. The time scale for the reorientation of Z-HT is estimated to be ca. 4 ps in cyclohexane assuming slip boundary conditions, in good agreement with the 5 ps decay of the absorption anisotropy.<sup>26</sup> The reorientation should be as fast or faster in the two alcohol solvents. The reorientation may be somewhat slower in hexadecane, but is still fast compared with the time scale for single bond isomerization. In addition, the  $=\text{CH}_2$  group displaced in the  $cZt \rightarrow tZt$  isomerization of hexatriene is much smaller than the phenyl group displaced in the isomerization of *trans*-stilbene. The change in volume may be estimated from the reaction coordinate calculations described above, with the prediction of a volume change no larger than 0.35% along the reaction coordinate. Because the reorientational diffusion is fast with respect to the  $cZt \rightarrow tZt$  isomerization, and the volume change is small, the molecule can easily reorient during the reaction. These observations are consistent with the insignificant viscosity dependence manifest in the data. It is unlikely that the frictional influence of viscous flow on this small volume change will have a substantial influence on the effective barrier height for this single bond isomerization reaction.

The excited-state  $trans \rightarrow p$  isomerization of stilbene is substantially faster in polar than in nonpolar solvents of comparable viscosity.<sup>58</sup> This effect has been attributed to the influence of the medium on the intrinsic barrier for activation and on the influence of solvation dynamics on the isomerization coordinate.<sup>52</sup> The barrier in the  $S_1$  state of *trans*-stilbene is generally attributed to an avoided crossing between electronic

states and it is relatively easy to imagine a mechanism by which solvent polarity could influence the barrier height. In contrast, the  $cZt \rightarrow tZt$  isomerization is a ground-state single bond rotation, albeit within the  $\pi$  framework of a conjugated polyene. The dipole moment of the molecule will vary as a function of the torsional angle although the variation is expected to be small.

The magnitude of the dipole moment of Z-HT calculated for both the RHF 6-63G\* and B3LYP/6-31G\*\* DFT calculations is plotted in Figure 8. The change in dipole moment along the reaction coordinate may provide a mechanism to modify the torsional potential in polar solvents. However, the change in the magnitude of the dipole moment is modest in the DFT calculation and even smaller in the RHF calculation. Although there is a change in direction as well as in magnitude of the dipole, fast solute reorientation will minimize the influence of the dipole direction on the activation energy. Rapid solvation by methanol (ca. 5 ps) and propanol (ca. 26 ps) will also serve to mitigate the influence of the change in dipole direction on the effective barrier for isomerization.<sup>59</sup>

**Conformational Relaxation  $cZt \rightarrow tZt$ -HT.** In the context of transition state theory the unimolecular rate constant for the  $cZt$ -HT  $\rightarrow$   $tZt$ -HT single bond isomerization is the canonical rate constant

$$k_{\text{TST}}(T) = \frac{k_{\text{b}}T}{h} \frac{Q_{\text{TS}}(T)}{Q_{\text{r}}(T)} e^{-E_{\text{a}}/k_{\text{b}}T} \quad (4)$$

where  $Q_{\text{TS}}$  and  $Q_{\text{r}}$  are the vibration/rotation partition functions for the transition state and the reactant respectively,  $k_{\text{b}}$  is the Boltzmann constant,  $T$  is the temperature, and  $E_{\text{a}}$  is the activation energy. Calculated vibrational frequencies for the  $cZt$  conformer and the transition state (RHF/6-31G\*\*) may be used to estimate  $A_{\text{h}}$  directly from eq 4 in the limit of harmonic potentials. These calculations yield values of  $A_{\text{h}} = 2.8\text{--}3.4 \times 10^{12} \text{ s}^{-1}$  for the temperature range investigated here. This is slightly lower than the value of  $A_{\text{h}}$  deduced from the measurements in alcohol solvents ( $A_{\text{h}} = 4 \times 10^{12} \text{ s}^{-1}$ ) but well within the error, which permits values ranging from  $1.5 \times 10^{12}$  to  $1 \times 10^{13} \text{ s}^{-1}$ .

In the absence of precise knowledge of the transition state, the expression in eq 4 is often used in a simplified form. Assuming that only the reactive coordinate differs between the ground state and the transition state, the expression for  $k_{\text{TST}}$  can be written as

$$k_{\text{TST}}(T) = \frac{k_{\text{b}}T}{h} [1 - e^{-h\nu_{\text{a}}/k_{\text{b}}T}] e^{-E_{\text{a}}/k_{\text{b}}T} \quad (5)$$

where  $\nu_{\text{a}}$  is the frequency of the effective reactive vibration. Under the assumption that the reactive coordinate will be a torsional vibration with a frequency of  $100\text{--}500 \text{ cm}^{-1}$ , the pre-exponential factor in eq 5 is estimated to be  $2.3\text{--}6.6 \times 10^{12} \text{ s}^{-1}$  over the temperature range from 283 to 353 K. An effective frequency of 125 to  $150 \text{ cm}^{-1}$  for the torsional coordinate reproduces the values calculated using eq 4. In the high-temperature limit where  $k_{\text{b}}T \gg h\nu_{\text{a}}$ , the polynomial expansion of  $e^{-h\nu_{\text{a}}/k_{\text{b}}T}$  in eq 5 leads to a simplified equation for the transition state rate constant where the exponential prefactor is independent of temperature

$$k_{\text{TST}}(T) = \nu_{\text{a}} e^{-E_{\text{a}}/k_{\text{b}}T} \quad (6)$$

According to Kramers' theory for unimolecular reactions in liquids the frictional influence of the environment should result in a rate constant given by

$$k = k_{\text{TST}}\kappa \quad (7)$$

where  $\kappa$  is the Kramers' transmission coefficient, which may be approximated as

$$\kappa = \left[ 1 + \left( \frac{\beta}{2\omega_{\text{a}}} \right)^2 \right]^{1/2} - \frac{\beta}{2\omega_{\text{a}}} \quad (8)$$

In this equation,  $\omega_{\text{a}}$  is the (imaginary) frequency describing the curvature of the barrier and  $\beta$  describes the friction of the solvent on the reactive motion.<sup>32,60,61</sup> In the high-friction limit ( $\beta > 2\omega_{\text{a}}$ ), the Kramers' coefficient reduces to  $\kappa = \omega_{\text{a}}/\beta$ .

In the Smoluchowski–Stokes–Einstein limit the friction on the reaction coordinate is related to the macroscopic shear viscosity of the solvent with  $\beta = \eta$ .<sup>32</sup> However, sublinear dependences of the rate constant for isomerization reactions on the solvent viscosity are commonly reported in the literature.<sup>39,45,46,62</sup> This sublinear dependence on viscosity leads to an equation for the transmission coefficient

$$\kappa = \frac{\omega_{\text{a}}}{\eta^{\gamma}} \quad (9)$$

where  $0 \leq \gamma \leq 1$ .<sup>41</sup> The parameter  $\gamma$  can be interpreted as the fraction of the activation energy for viscous flow that acts as a friction on the reaction coordinate.<sup>48</sup>

In the limit of medium friction ( $\beta \ll 2\omega_{\text{a}}$ ) the Kramers' coefficient in eq 8 will approach unity. Thus  $\kappa$  is always less than or equal to one in the presence of environmental friction. It is never predicted to be greater than one. A generalization of this equation with a frequency dependent friction was put forth by Grote and Hynes.<sup>63–65</sup> However, in Grote–Hynes theory, the transmission coefficient will still be less than 1.

The range of values for  $A_{\text{h}}$  estimated by transition state theory for  $cZt \rightarrow tZt$  single bond isomerization is an order of magnitude lower than the value of  $6 \times 10^{13} \text{ s}^{-1}$  determined from the data obtained in alkane solvents. As transition-state theory should provide an upper limit for the reaction rate in the region of moderate to high friction, where rapid energy randomization is guaranteed, this result provides a significant puzzle. Interestingly, Schroeder et al. also report an order of magnitude deviation between the calculated and experimental rate constant of *trans*-stilbene in low viscosity polar solvents, with the experimental rate faster than predicted by transition state theory. This is not a universal phenomena however as *trans*-stilbene was the only system observed to exhibit this anomalous behavior, while good agreement between calculated and predicted rates was reported for several larger systems.<sup>57</sup> Sun et al. also comment on an observed " $k_{\text{TST}}$ " for the  $\text{trans} \rightarrow \text{p}$  isomerization of stilbene in alkane solvents larger than the  $k_{\text{TST}}$  calculated by eq 6 with an anticipated torsional frequency of  $\nu = 100 \text{ cm}^{-1}$ . Although only the difference reported by Sun et al. is only a factor of 2.5, not the order of magnitude found here for Z-HT.<sup>50</sup>

The value of  $A_{\text{h}}$  in alcohol solvents is systematically lower than the value in simple alkanes, falling within the range of values consistent with transition state theory. The difference observed between the alkane and alcohol solvents may suggest an additional frictional dependence of  $A_{\text{h}}$  for the alcohol solvent, which is not present in simple alkanes. However, this friction is not simply related to the solvent shear viscosity; in fact the most striking feature of the data is the complete lack of dependence of the reaction rate on the solvent shear viscosity. Over the range of temperatures investigated the ratio of viscosities in like solvents range from 2 to 5 with no apparent

effect on the reaction rate. This is apparent for the alkane data as illustrated in the inset to Figure 5 and is also true of the two alcohol solvents. In one specific example, the measured rate constants in methanol and propanol at 10 °C are 2.6 and 2.7 ns<sup>-1</sup>, respectively, despite a 4-fold increase in the solvent viscosity from 0.7 to 2.9 mPa s.

It seems likely that the correspondence between the transition-state rate value for  $A_h$  and the observed value in alcohol solvents reflects the general validity of transition-state theory and the discrepancy observed for alkane solvents identifies an additional contribution to the transition state partition function not yet accounted for. In the context of transition-state theory, a higher value for  $A_h$  requires a larger partition function for the transition state or a smaller partition function for the reactant minimum. It is interesting to speculate that this difference is related to intermolecular packing of the solvent. One potential source is a close-packing interaction between Z-HT and the alkane solvents resulting in a solvent-induced confinement term at the cZt minimum correlated with a corresponding increase in entropy of the transition state. This is not observed in alcohols where the hydrogen bonding interactions between solvent molecules decrease the confinement.

**Thermalization of hot Z-HT Formed from CHD.** The overall thermalization of Z-HT following internal conversion from the excited electronic state may be analyzed in the context of an internal temperature of the molecule and the potential surface for conformational relaxation as developed earlier.<sup>17</sup> In this formalism, the internal temperature of the molecule decays exponentially from the initial temperature  $T_{\max}$  representing a Boltzmann redistribution of the available energy introduced by the photon throughout the vibrational modes of Z-HT to the temperature of the bulk sample,  $T_{\text{sample}}$

$$T(t) = (T_{\max} - T_{\text{sample}})e^{-t/\tau_{\text{vib}}} + T_{\text{sample}} \quad (10)$$

Because the temperature varies as the Z-HT relaxes, the rate constants for conversion between the isomers are a function of time.

In the context of the conformational isomerization of Z-HT it is also important to keep track of the degeneracies of the various conformations and transition states. The planar tZt conformer is nondegenerate, while there are four cZt conformations and two distinct cZc conformations. A schematic of the potential energy landscape is illustrated in Figure 8. These degeneracies will influence the ratio of the transition state to reactant partition functions in eq 4.

The conformational relaxation and thermalization of Z-HT may be modeled using eqs 4, 5, and 8 to calculate the transition-state rate constants as a function of time. This model requires relative energies for the cZt and cZc conformers and for the transition states TS1 and TS2. In addition, the effective torsional frequencies corresponding to the reaction coordinates are required. By assumption that the relative energies of the conformers are approximated well in calculated potentials, cZt is ca. 1100–1300 cm<sup>-1</sup> above the tZt minimum, while cZc is ca. 2950–3450 cm<sup>-1</sup> above the tZt minimum. The cZt energy is in reasonable agreement with both calculated<sup>37,38</sup> and experimental (2.95 kcal/mol,<sup>66</sup> 2.81 kcal/mol<sup>36</sup>) values for the energy of the stable *cis*-like configuration of butadiene approximately 1000 cm<sup>-1</sup> above the *trans* configuration. The torsional frequency corresponding to the reaction coordinate is ca. 150 cm<sup>-1</sup> in the cZt and tZt conformations as described above. The experimental barriers for the cZt → tZt isomerization are 1450 and 1950 cm<sup>-1</sup> in alcohol and alkane solvents, respectively.

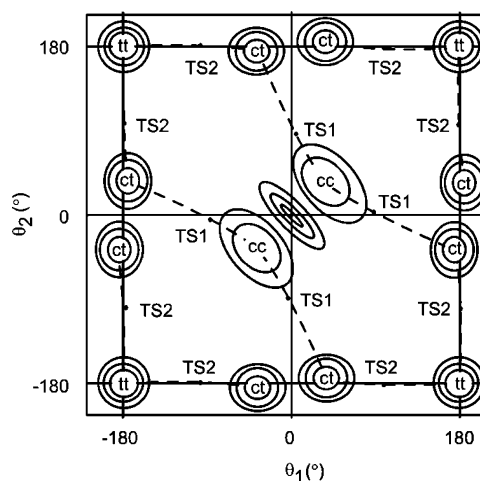


**Figure 9.** Schematic diagram of the potential-energy landscape for the conformers of Z-HT obtained by rotation about the two single bonds. The tZt conformer is planar while the cZt and cZc conformers are nonplanar. The cZc conformer exists in two helical conformations separated by a potential barrier caused by the steric interaction of the CH<sub>2</sub> groups, indicated by the blue contours. The cZt conformer exhibits four minima which may be distinguished by the direction of rotation about each of the single bonds. The transition states for cZt → tZt (TS2) and cZc → cZt (TS1) are indicated on the plot, as are approximate reaction coordinates (green dashed line). A more complete energy surface is provided by Hensler et al.<sup>22</sup>

The parameters for the cZc → cZt isomerization are less certain but may be estimated from quantum chemical calculations. The barrier for the cZc → cZt reaction is calculated to be 350–400 cm<sup>-1</sup>.<sup>22,26</sup> The effective torsional frequency is estimated at ca. 75 cm<sup>-1</sup> from the ratio of partition functions for TS1 and cZc using harmonic frequencies from RHF 6/31G calculations.<sup>17,26</sup> This value of  $\nu_a$  is significantly less than  $k_bT$  over the entire temperature range of the evolution (2000 to ca. 300 K). Thus it is useful to make a high-temperature approximation for the transition state rate constant. The rate constant for the cZc → cZt reaction can be approximated as

$$k_{cZc \rightarrow cZt}(T) = \nu_a k e^{-E_a/k_bT} = \alpha e^{-E_a/k_bT} \quad (11)$$

where  $\alpha$  is a fitting parameter taking into account both the torsional frequency and the friction on the reaction coordinate. Unless the decay of the internal temperature of the molecule is relatively fast compared with the lifetime of the cZc conformer,  $k_{cZc \rightarrow cZt}$  will be constant ( $E_a \ll kT$  at early times) and  $\alpha$  will be a fitting parameter describing time-independent rate constant for conformational relaxation of hot cZc-HT.

In the context of this theory, the evolution of the conformer population in all four solvents may be modeled with three fitting parameters,  $\alpha$ ,  $k_{cZt \rightarrow tZt}$ , and  $\tau_{\text{vib}}$ . The results of this analysis are plotted in Figure 10.

The parameters obtained from the fit of this model to the data are  $\alpha = 3.3 \times 10^{11} \text{ s}^{-1}$  in alcohols and  $1.3 \times 10^{11} \text{ s}^{-1}$  in alkanes,  $k_{cZt \rightarrow tZt} = 10$  in alcohols and 20 in alkanes,  $\tau_{\text{vib}} = 12$  ps in cyclohexane, 20 ps in hexadecane, 5 ps in methanol, and 6 ps in propanol. As illustrated in Figure 10, this parameter set does a very good job of fitting the overall trends seen in the data.

There are three key observations here:

(1) The friction of the environment on the initial evolution from cZc-HT to cZt-HT is about a factor of 2–3 higher in alkane solvents than in alcohol solvents. The precise interpretation of this is unclear as a transition-state approach is inappropriate. The barrier for the isomerization is somewhat uncertain, but it

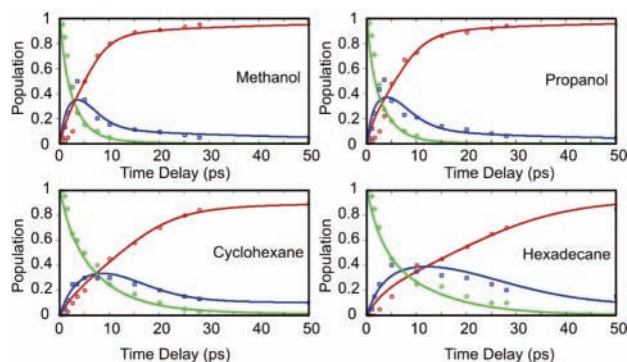


**Figure 10.** Population dynamics of cZc (green), cZt (blue), and tZt (red) hexatriene as a function of time following excitation of CHD. The points are the populations extracted from the data as described above while the lines were obtained by solving the coupled differential equations describing the populations as a function of time.

is likely that the vibrationally hot molecule has substantial population in energy levels above the barrier at early times. When the calculated barrier of  $400\text{ cm}^{-1}$  is assumed, the exponential term in eq 11 is slowly varying between about 0.5 and 0.75 as Z-HT cools from 2000 to 1000 K. Thus the analysis simply reproduces the observed nearly exponential decays of ca. 2 and 6 ps for the relaxation of hot cZc-HT. That is:  $[3.3 \times 10^{11}\text{ s}^{-1} \times 0.67 \times 2]^{-1} = 2.3\text{ ps}$ ,  $[1.3 \times 10^{11}\text{ s}^{-1} \times 0.67 \times 2]^{-1} = 5.7\text{ ps}$ .

(2) The “friction” coefficient on the cZt to tZt isomerization is greater than one, implying that transition state theory as implemented underestimates the rate constant. This is consistent with analysis of the thermal cZt to tZt reaction discussed above. In fact the value for  $\kappa_{\text{cZt} \rightarrow \text{tZt}} = 20$  in alkane solvents is in excellent agreement with the ratio of the experimental Arrhenius prefactor to the transition state theory estimate ( $6 \times 10^{13}\text{ s}^{-1}/3 \times 10^{12}\text{ s}^{-1} = 20$ ) obtained for the thermal cZt  $\rightarrow$  tZt reaction. The value of  $\kappa_{\text{cZt} \rightarrow \text{tZt}}$  in alcohols is smaller than that in alkanes, but the difference is only a factor of 2, not an order of magnitude as observed for the thermal reaction. Perhaps the energy removed from the hot solute at early times transiently heats the surrounding solvent and reduces the friction on the reactive motion or collapses the solvent around the solute into closer packing, i.e., into a situation similar to the alkanes.

(3) The time scale for the vibrational relaxation is somewhat dependent on the solvent and approximately a factor of 2 faster in the alcohol solvents than in cyclohexane. This is consistent with a stronger interaction between the Z-HT solute and the surrounding solvent in alcohols than in alkanes. The values obtained here are in good agreement with those reported earlier.<sup>17,20</sup>

## V. Conclusions

This paper reports a careful comparison of the conformational relaxation dynamics of Z-HT in alkane and alcohol solvents. These data confirm the earlier observation that the relaxation and thermalization of hot Z-HT is much faster in alcohol solvents than in alkane solvents. The solvent influence is related to the nature of the alcohol vs alkane solvent but is not related in any simple fashion to the macroscopic solvent shear viscosity. A measurement of the temperature-dependent cZt  $\rightarrow$  tZt isomerization highlights two aspects of the solvent dependence. First, the barrier for the cZt  $\rightarrow$  tZt conformational isomerization is influenced by the solvent, and is 25% lower in alcohols (ca.  $1450\text{ cm}^{-1}$ ,  $17.4\text{ kJ/mol}$ ) than in alkanes (ca.  $1950\text{ cm}^{-1}$ ,  $23.5\text{ kJ/mol}$ ). In addition, the equilibrium Arrhenius prefactor,  $A_h$ ,

is an order of magnitude smaller for alcohols (ca.  $4 \times 10^{12}\text{ s}^{-1}$ ) than alkanes (ca.  $6 \times 10^{13}\text{ s}^{-1}$ ) and is independent of the solvent viscosity. These values for  $A_h$  provide something of a conundrum as the value in alkane solvents is an order of magnitude larger than that predicted by simple transition-state theory. The difference cannot be easily attributed to an activated viscous friction on the reactive motion as the data is independent of solvent viscosity. A similar, as yet unexplained, phenomenon was reported for *trans*-stilbene in the low viscosity solvent liquid ethane.<sup>57</sup>

The relaxation of hot Z-HT produced by the photochemical ring-opening reaction of CHD evolves from the conformationally strained cZc-HT form to the more stable cZt-HT form on a time scale of 2 ps in alcohols and 6 ps in alkanes but is not dependent on the particular alkane or alcohol solvent. The overall decay of the internal vibrational temperature of the hot Z-HT is faster in alcohols (5–6 ps) than alkanes (12–20 ps) and is dependent on the specific solvent investigated.

**Acknowledgment.** This research was funded by the NSF through Grant CHE-0078972. The authors would like to thank Professor Arthur Ashe for his valuable advice and assistance in the synthesis and purification of *cis*-hexatriene and Professor Eitan Geva for useful discussions.

## References and Notes

- (1) Minnaard, N. G.; Havinga, E. *Rec. Trav. Chim.* **1973**, *92*, 1315–1320.
- (2) Trulson, M. O.; Dollinger, G. D.; Mathies, R. A. *J. Am. Chem. Soc.* **1987**, *109*, 586–587.
- (3) Reid, P. J.; Doig, S. J.; Mathies, R. A. *Chem. Phys. Lett.* **1989**, *156*, 163–168.
- (4) Trulson, M. O.; Dollinger, G. D.; Mathies, R. A. *J. Chem. Phys.* **1989**, *90*, 4274–4281.
- (5) Celani, P.; Ottani, S.; Olivucci, M.; Bernardi, F.; Robb, M. A. *J. Am. Chem. Soc.* **1994**, *116*, 10141–10151.
- (6) Reid, P. J.; Lawless, M. K.; Wickham, S. D.; Mathies, R. A. *J. Phys. Chem.* **1994**, *98*, 5597–5606.
- (7) Hayden, C. C.; Chandler, D. W. *J. Phys. Chem.* **1995**, *99*, 7897–7903.
- (8) Pullen, S. H.; Walker II, L. A.; Donovan, B.; Sension, R. J. *Chem. Phys. Lett.* **1995**, *242*, 415–420.
- (9) Celani, P.; Bernardi, F.; Robb, M. A.; Olivucci, M. *J. Phys. Chem.* **1996**, *100*, 19364–19366.
- (10) Fuss, W.; Schikarski, T.; Schmid, W. E.; Trushin, S.; Kompa, K. L. *Chem. Phys. Lett.* **1996**, *262*, 675–682.
- (11) Ohta, K.; Naitoh, Y.; Saitow, K.; Tominaga, K.; Hirota, N.; Yoshihara, K. *Chem. Phys. Lett.* **1996**, *256*, 629–634.
- (12) Fuss, W.; Schikarski, T.; Schmid, W. E.; Trushin, S. A.; Hering, P.; Kompa, K. L. *J. Chem. Phys.* **1997**, *106*, 2205–2211.
- (13) Garavelli, M.; Celani, P.; Fato, M.; Bearpark, M. J.; Smith, B. R.; Olivucci, M.; Robb, M. A. *J. Phys. Chem. A* **1997**, *101*, 2023–2032.
- (14) Kauffmann, E.; Frei, H.; Mathies, R. A. *Chem. Phys. Lett.* **1997**, *266*, 554–559.
- (15) Lochbrunner, S.; Fuss, W.; Kompa, K. L.; Schmid, W. E. *Chem. Phys. Lett.* **1997**, *274*, 491–498.
- (16) Trushin, S. A.; Fuss, W.; Schikarski, T.; Schmid, W. E.; Kompa, K. L. *J. Chem. Phys.* **1997**, *106*, 9386–9389.
- (17) Anderson, N. A.; Pullen, S. H.; Walker, L. A., II; Shiang, J. J.; Sension, R. J. *J. Phys. Chem. A* **1998**, *102*, 10588–10598.
- (18) Pullen, S. H.; Anderson, N. A.; Walker, L. A., II; Sension, R. J. *J. Chem. Phys.* **1998**, *108*, 556–563.
- (19) Ohta, K.; Naitoh, Y.; Tominaga, K.; Hirota, N.; Yoshihara, K. *J. Phys. Chem. A* **1998**, *102*, 35–44.
- (20) Lochbrunner, S.; Fuss, W.; Schmid, W. E.; Kompa, K. L. *J. Phys. Chem. A* **1998**, *102*, 9334–9344.
- (21) Henseler, D.; Auer, A.; Hohlneicher, G. *J. Inform. Rec.* **1998**, *24*, 123–127.
- (22) Henseler, D.; Rebentisch, R.; Hohlneicher, G. *Int. J. Quantum Chem.* **1999**, *72*, 295–305.
- (23) Anderson, N. A.; Durfee, C. G.; Murnane, M. M.; Kapteyn, H. C.; Sension, R. J. *Chem. Phys. Lett.* **2000**, *322*, 365–371.
- (24) Fuss, W.; Schmid, W. E.; Trushin, S. A. *J. Chem. Phys.* **2000**, *112*, 8347–8362.

- (25) Garavelli, M.; Page, C. S.; Celani, P.; Olivucci, M.; Schmid, W. E.; Trushin, S. A.; Fuss, W. *J. Phys. Chem. A* **2001**, *105*, 4458–4469.
- (26) Pullen, S. H.; Anderson, N. A.; Walker, L. A., II; Sension, R. J. *J. Chem. Phys.* **1997**, *107*, 4985–4993.
- (27) Braun, M.; Fuss, W.; Kompa, K. L.; Wolfrum, J. *J. Photochem. Photobiol. A* **1991**, *61*, 15–26.
- (28) Fuss, W.; Hofer, T.; Hering, P.; Kompa, K. L.; Lochbrunner, S.; Schikarski, T.; Schmid, W. E. *J. Phys. Chem.* **1996**, *100*, 921–927.
- (29) Fuss, W.; Lochbrunner, S. *J. Photochem. Photobiol. A* **1997**, *105*, 159–164.
- (30) Anderson, N. A.; Shiang, J. J.; Sension, R. J. *J. Phys. Chem. A* **1999**, *103*, 10730–10736.
- (31) Anderson, N. A.; Sension, R. J. Solvent dependence of excited-state lifetimes in 7-dehydrocholesterol and simple polyenes. In *Liquid Dynamics: Experiment, Simulation, and Theory*; Fourkas, J., Ed.; American Chemical Society: Washington, DC, 2002; pp 148–158.
- (32) Hanggi, P.; Talkner, P.; Borkovec, M. *Rev. Mod. Phys.* **1990**, *62*, 251–341.
- (33) Viscosity of Liquids. In *CRC Handbook of Chemistry & Physics, Internet Version*, 86th ed.; Lide, D. R., Ed.; Taylor and Francis: Boca Raton, FL, 2006.
- (34) Hwa, J. C. H.; Debenneville, P. L.; Sims, H. J. *J. Am. Chem. Soc.* **1960**, *82*, 2537–2540.
- (35) Ackerman, J. R.; Kohler, B. E. *J. Chem. Phys.* **1984**, *80*, 45–50.
- (36) Engeln, R.; Consalvo, D.; Reuss, J. *J. Chem. Phys.* **1992**, *160*, 427–433.
- (37) Karpfen, A.; Parasuk, V. *Mol. Phys.* **2004**, *102*, 819–826.
- (38) Fabiano, E.; Della Sala, F. *Chem. Phys. Lett.* **2006**, *418*, 496–501.
- (39) Rothenberger, G.; Negus, D. K.; Hochstrasser, R. M. *J. Chem. Phys.* **1983**, *79*, 5360–5367.
- (40) Sundstrom, V.; Gillbro, T. *Chem. Phys. Lett.* **1984**, *109*, 538–543.
- (41) Courtney, S. H.; Fleming, G. R. *J. Chem. Phys.* **1985**, *83*, 215–222.
- (42) Lee, M. Y.; Holtom, G. R.; Hochstrasser, R. M. *Chem. Phys. Lett.* **1985**, *118*, 359–363.
- (43) Balk, M. W.; Fleming, G. R. *J. Phys. Chem.* **1986**, *90*, 3975–3983.
- (44) Courtney, S. H.; Balk, M. W.; Philips, L. A.; Webb, S. P.; Yang, D.; Levy, D. H.; Fleming, G. R. *J. Chem. Phys.* **1988**, *89*, 6697–6707.
- (45) Kim, S. K.; Fleming, G. R. *J. Phys. Chem.* **1988**, *92*, 2168–2172.
- (46) Kim, S. K.; Courtney, S. H.; Fleming, G. R. *Chem. Phys. Lett.* **1989**, *159*, 543–548.
- (47) Lee, M. Y.; Haseltine, J. N.; Smith, A. B.; Hochstrasser, R. M. *J. Am. Chem. Soc.* **1989**, *111*, 5044–5051.
- (48) Saltiel, J.; Sun, Y. P. *J. Phys. Chem.* **1989**, *93*, 6246–6250.
- (49) Sun, Y. P.; Saltiel, J. *J. Phys. Chem.* **1989**, *93*, 8310–8316.
- (50) Sun, Y. P.; Saltiel, J.; Park, N. S.; Hoburg, E. A.; Waldeck, D. H. *J. Phys. Chem.* **1991**, *95*, 10336–10344.
- (51) Schroeder, J.; Troe, J.; Vohringer, P. *Chem. Phys. Lett.* **1993**, *203*, 255–260.
- (52) Waldeck, D. H. *J. Mol. Liq.* **1993**, *57*, 127–148.
- (53) Schroeder, J.; Schwarzer, D.; Troe, J.; Vohringer, P. *Chem. Phys. Lett.* **1994**, *218*, 43–50.
- (54) Schroeder, J.; Troe, J.; Vohringer, P. *Z. Phys. Chem.* **1995**, *188*, 287–306.
- (55) Meyer, A.; Schroeder, J.; Troe, J.; Votsmeier, M. *J. Photochem. Photobiol.* **1997**, *105*, 345–352.
- (56) Meyer, A.; Schroeder, J.; Troe, J. *J. Phys. Chem. A* **1999**, *103*, 10528–10539.
- (57) Schroeder, J.; Steinel, T.; Troe, J. *J. Phys. Chem. A* **2002**, *106*, 5510–5516.
- (58) Kim, S. K.; Courtney, S. H.; Fleming, G. R. *Chem. Phys. Lett.* **1989**, *159*, 543.
- (59) Maroncelli, M. *J. Chem. Phys.* **1997**, *106*, 1545–1555.
- (60) Chandrasekhar, S. *Rev. Mod. Phys.* **1943**, *15*, 1–89.
- (61) Kramers, H. A. *Physica* **1940**, *7*, 284–304.
- (62) Akesson, E.; Hakkarainen, A.; Laitinen, E.; Helenius, V.; Gillbro, T.; Korppi-Tommola, J.; Sundstrom, V. *J. Chem. Phys.* **1991**, *95*, 6508–6523.
- (63) Grote, R. F.; Hynes, J. T. *J. Chem. Phys.* **1981**, *74*, 4465–4475.
- (64) Grote, R. F.; Vanderzwan, G.; Hynes, J. T. *J. Phys. Chem.* **1984**, *88*, 4676–4684.
- (65) Grote, R. F.; Hynes, J. T. *J. Chem. Phys.* **1980**, *73*, 2715–2732.
- (66) Saltiel, J.; Sears, D. F.; Turek, A. M. *J. Phys. Chem. A* **2001**, *105*, 7569–7578.